

PERFORMANCE ANALYSIS AND THERMODYNAMIC MODELING OF A POLY GENERATION SYSTEM BY INTEGRATING A MULTI-EFFECT-DESALINATION THERMO-VAPOR COMPRESSION (MED-TVC) SYSTEM WITH A COMBINED COOLING, HEATING AND POWER (CCHP) SYSTEM

H. Ghaebi^{1,*}, G. Abbaspour¹

ABSTRACT

In the present study, performance analysis of a multi effect distillation with thermos vapor compressor (MED-TVC) desalination system coupled to a combined cooling, heating and power (CCHP) system with gas turbine prime mover has been carried out to cogeneration of cooling, heating, power and potable water. The system incorporates air compressor, combustion chamber, gas turbine, triple pressure heat recovery system generator (HRSG), absorption chiller and MED-TVC. A thermodynamic modeling based on mass and energy balance equations is applied for each component of the integrated system. The engineering equation solver (EES) software was used for modeling. It is found that the efficiency of the integrated system reached to 84% (the efficiency of the gas turbine cycle was 32%). Furthermore, a parametric study has been presented in order to investigate the effects of the operational parameters on the performance of the integrated system.

Keywords: Desalination, CCHP, Gas turbine, MED-TVC, Thermodynamic analysis

INTRODUCTION

Energy and energy saving are one of the crucial items all around the world. Problems with energy supply and its use are related not only to global warming, but also to environmental concerns such as air pollution, acid precipitation, ozone depletion, forest destruction and emission of radioactive substances [1]. These issues must be taken into our consideration simultaneously if humanity is to achieve a bright energy future with minimal environmental impacts [2-4].

Cogeneration is one of the best energy saving methods to make a more efficient usage of fuels and achieve environmental improvements. Cogeneration makes it possible to produce electricity and useful thermal energy from the same energy resource. The requirements of cogeneration may be met in many ways, such as steam and gas turbines, fuel cells and Sterling engines [5-6]. A part of heat production of a site may be used for handling an absorption chiller and thereby the cooling demand of the site will be covered and/or for operating a desalination plant to produce fresh water. In fact, in such a case the most beneficial way to use primary energy is applied, because it makes system possible to produce power, heat, cold and fresh water simultaneously.

Water exists in huge amount on earth but only a small fraction has suitable conditions for drinking and irrigation [7]. Desalination is one of the most important processes to provide water to population in water scarcity areas. But desalination processes consume a lot of energy that unfortunately the majority of their energy requirements is obtained from oil or natural gas [8].

Today, distillation and membrane methods are the two main seawater desalination processes. Among these methods, multi stage flash (MSF), multi effect distillation (MED), vapor compression (VC) and reverse osmosis (RO) are suitable for the large and medium capacity of freshwater production [9]. MSF and MED seawater desalination systems are suitable for being coupled with power plants because they could utilize the waste heat from power cycle for improving the fuel efficiency of the whole plants. In the other words, they usually use the waste energy of flue gas (which is emitted from gas turbine cycles) and extracted vapor of steam turbines or heat recovery steam generator (HRSG). Compared with the most widely used MSF desalination, MED and multi effect distillation thermal vapor compression (MED-TVC) have the advantages of lower corrosion and scaling rates, lower capital cost, longer operation life and less pumping power consumption [10].

So far, many researchers have studied dual purpose (combined power and water) plants. Johansen et al [11] evaluated four combined heat and power (CHP) plants coupled to several desalination processes. They showed

This paper was recommended for publication in revised form by Regional Editor Omid Mahian

¹ Department of Mechanical Engineering, Faculty of Engineering, University of Mohaghegh Ardabili, P.O.B 179, Ardabil, IRAN

*E-mail address: hghaebi@uma.ac.ir

Manuscript Received 28 December 2016, Accepted 11 March 2017

that by using a gas turbine, an HRSG and a back pressure steam turbine together with a MED-RO desalination system, high effective energy utilization can be achieved.

Wade [12] reviewed energy and cost allocation methods in dual purpose plant of power and desalination. He studied the integration of gas turbine power plants and CHP cycles with RO and MSF desalination plants. Cardona and Piacentino [13] optimized a combined cycle with both production of electricity and fresh water from the exergo-economics point of view. Their study involved a combination of RO and MSF desalination systems in which exhaust waste energy from the power cycle entered to the MSF section and also power was supplied to the RO section and MSF auxiliary equipment. Darwish and Najem [14] proposed using gas turbine with RO and MSF desalination units for efficient usage of the same energy source. Rensonnet et al [15] carried out thermoeconomic analysis of different configurations of gas turbine dual purpose power and desalination and also hybrid plants. They modeled combined Gas turbine with RO, combined cycle with RO, combined cycle with MED and a hybrid plant arrangement combining combined cycle, MED and RO. Wang and Lior [16-17] presented a thermodynamic model for integrated MED-TVC and humidified gas turbine cycle. Chacartegui [18] considered the performance of a cogeneration plant – combined power plant and desalination – with a stationary lumped volume model. Khoshgoftar Manesh and Amidpour [19] applied an evolutionary algorithm to multi-objective thermoeconomic optimization of coupling MSF plant with a pressurized water reactor (PWR) nuclear power plant. Ansari et al [20] carried out thermoeconomic optimization of a typical PWR plant coupled to a MED-TVC desalination system. They used Total Revenue Requirement (TRR) method for economic analysis. Hosseini et al [21] investigated the effects of equipment reliability in thermoeconomic analysis of a combined power and MSF water desalination plant. In the other research, Hosseini et al [22] performed cost optimization of a dual production plant considering exergetic, environmental and reliability concepts. Shakib et al [23] studied thermodynamic and economic aspects of MED-TVC. The MED-TVC was combined with gas turbine power plants, an Alstom GE13E plant that had stood at the south of Iran, near seashore, and had a nominal output power of 165 MW. In the other research [24], they performed an optimization using two heuristic algorithms, namely, genetic algorithm (GA) and particle swarm optimization (PSO). Esfahani and Yoo [25] conducted a feasibility study of an integrated system comprising a steam injected gas turbine and MED-TVC. Almutairi et al. [26] carried out energetic and exergetic analysis of a gas turbine integrated with ME-TVC-MED system. They concluded that by increasing of the compressor pressure ratio and feed water temperature, the efficiency of the combined system improved. Hanafi et al [27] performed thermoeconomic analysis of a combined gas turbine MED-TVC system. Their results showed that the production cost of the power and potable water is 20.6 % less than their standalone production. Sanaye and Asgari [28] modeled, analyzed and optimized an integrated gas-turbine combined-cycle power plant with Multi-stage Flash (MSF) desalination unit using multi-objective genetic algorithm method.

However, to our knowledge, no previous investigation has proposed or assessed the integration of MED-TVC with gas turbine based CCHP plant. The sub-objectives of this research paper are multi-fold, and include:

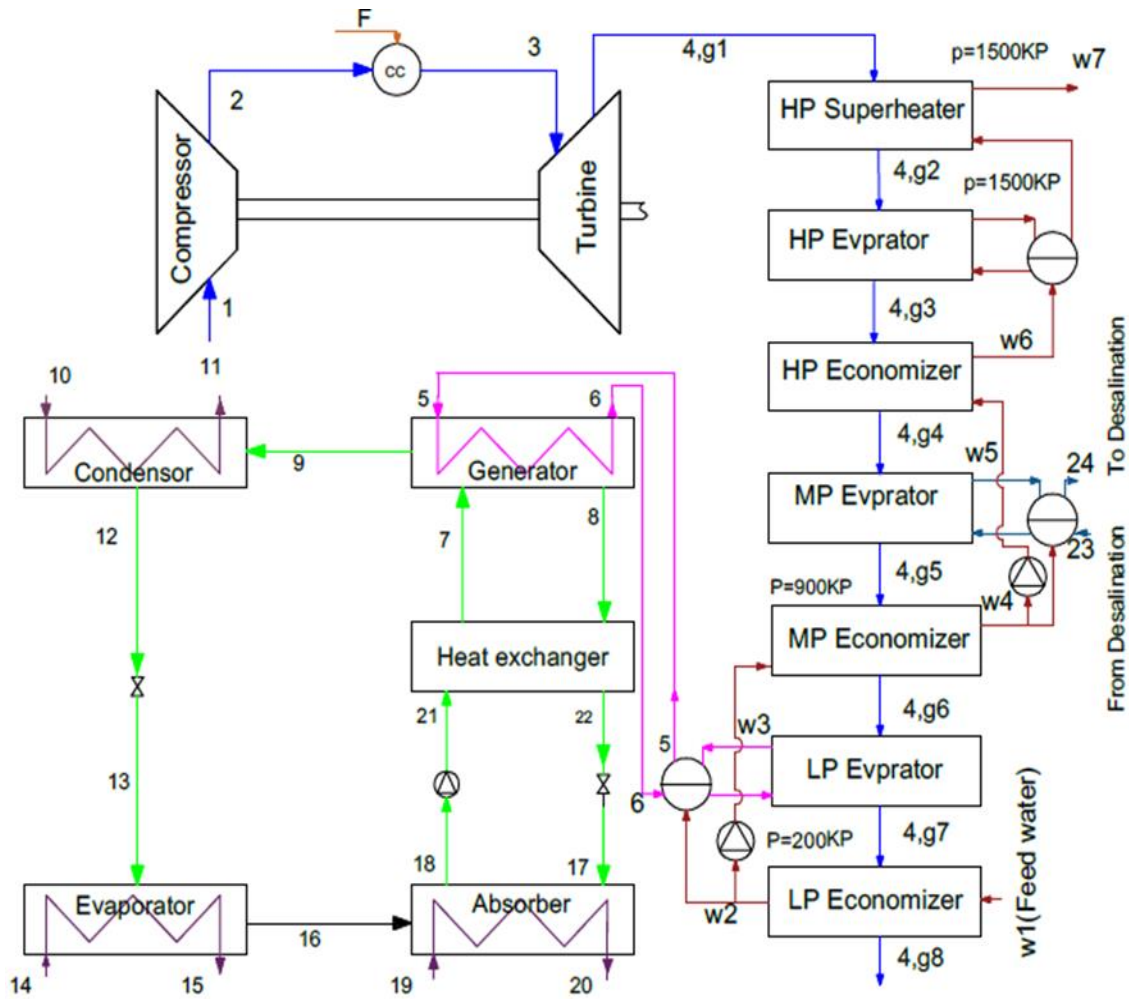
- To develop a novel configuration of gas turbine based CCHP plant integrated with MED-TVC to combined cooling, heating, power and potable water.
- To consider a triple pressure HRSG to produce steam in three levels.
- To comprehensively thermodynamic model of the proposed system.
- To perform parametric study to see the effect of variations of operating parameters on the performance of the integrated system.

SYSTEM DESCRIPTION

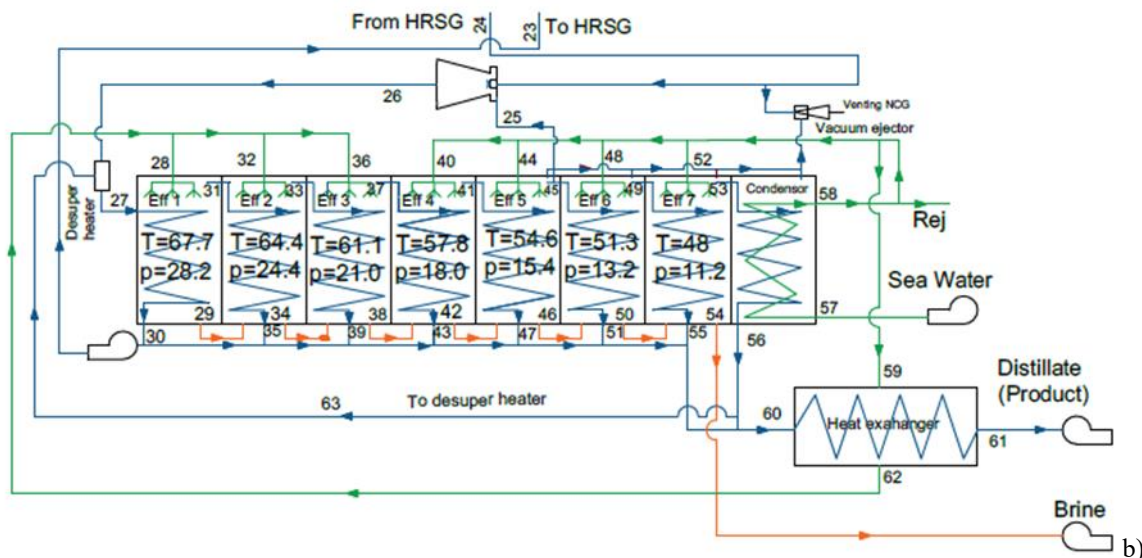
The schematic diagram of the proposed system is shown in Fig.1. This plant consists of air compressor, combustion chamber, gas turbine, triple-pressure HRSG, lithium bromide-water absorption chiller and MED-TVC.

Ambient air enters the air compressor at point (1) and, after compression at point (2), it leaves compressor. This hot air enters combustion chamber at point (2) which is fueled by fuel injected into the combustion chamber at point (F). After combustion reaction, hot exhaust gas is produced at point (3). Next, the hot gases leaving combustion chamber are expanded through a gas turbine to produce power. At point (4) hot flue gases leave gas turbine and enter heat recovery steam generator (HRSG) in which energy of flue gases is being utilized to produce steam. Here we used triple pressure HRSG to produce steam in three levels (saturated low pressure (LP) steam, saturated medium pressure (MP) steam and superheated high pressure (HP) steam). The LP steam is used to run a single effect LiBr – H₂O absorption chiller for cooling purpose. This steam supplied to generator of absorption

chiller at point (5) and after heat transfer to LiBr – H₂O solution, comes back to LP evaporator of HRSG at point (6). Because of heat transfer to LiBr – H₂O, the refrigerant (H₂O) is separated from LiBr – H₂O in the generator and goes through the condenser at point (5) and evaporator at state (13) through the expansion valve at state (12).



a)



b)

Figure 1. Schematic diagram of the integrated system, a) gas turbine cycle with HRSG and absorption chiller b) MED-TVC desalination plant

The water vapor after boiling in evaporator enters the absorber at point (16). In the absorber, it mixes with weak solution that enters absorber at point (17) and its heat is rejected by cooling water (19-20). The strong solution leaves the absorber at point (18) and pumped to the pressure of the point (21). This strong and high pressure solution is heated through heat exchanger and enters generator at point (7). The exhaust weak and high pressure solution of heat exchanger enters absorber at point (17) after pressure drop through expansion valve.

The saturated MP steam is used to run a MED-TVC desalination plant. The main components of that are the steam ejector (which acts as the heart of the system), falling film evaporators (effects) and a condenser (Fig.1b). The saturated steam which is fed from HRSG enters steam ejector at point (24) and after mixing with the return steam from the n^{th} effect (point (25)) expands to the pressure of the first effect at point (26). This steam is converted to superheated steam because of expansion and it needs to become saturated steam to enter the first effect. Then a de-superheater is used in that a part of leaving fresh water from the last effect is mixed with the superheated steam (point (26)) to convert to saturated steam (point (27)). The saturated steam enters the first effect and rejects its latent heat to the sea water and condenses and a part of it (equal of the amount of the steam that fed from HRSG) returns to HRSG by a pump. The remainder joints to the fresh water line. The vapor formed in the first effect (point (31)) is directed to the second effect. Another part of the seawater that is named brine (point (29)) enters the next effect. The vapor generated in each effect is passed through demisters and enters the next effect to transfer heat to the feed seawater. This trend is continued all over the effects and the heat of the last effect is absorbed by condenser and used to preheat the seawater. The brine is collected from all of the effects and rejected to sea (point (54)). Also a heat exchanger is used to preheat the feed seawater that enters the first three effect (point (62)). The fresh water is left at the desired temperature at point (61).

Feed-water preheating has two advantages: the first one is preheating of the feed for the effects number 1, 2 and 3, which leads to reduction of the total energy consumption and exergy destruction, the second advantage is reduction of the product water temperature which reduces the amount of exergy loss to environment.

The superheated HP steam that is generated by the HP evaporator of the HRSG will be utilized as process steam, directly (point (w_7)).

Thermodynamic Analysis

The energy analysis is presented in this section. Engineering Equation Solver (EES) is used as the main software for all calculations. For thermodynamic analysis, the principles of mass and energy conservations are applied to each system component. The following assumptions are considered in this work:

- All processes are considered to be working as state and steady flow.
- The volumetric composition of the inlet air is 75.98% N₂, 20.18% O₂, 0.03% CO₂ and 3.81% H₂O [29].
- Pressure drop along the HRSG and combustion chamber is supposed to be 5% and 3%, respectively [5].
- The fuel is methane with a low heating value of 50,010 kJ/kg [5].
- Air compressor and gas turbine are considered adiabatic [5].
- There is no pressure drop heat loss in pipelines.
- There is no heat loss in absorption chiller and MED-TVC components [24].
- Vapor formed in each effect is free of salt [24].
- Final reject salinity is assumed 70000 ppm [24].
- Heat transfer area of evaporators 2 to N is the same [24].

The following equations are the energy balance for the components of the system:

Gas Turbine Cycle

To calculate the air compressor efficiency (η_c) Equation (1) is used, which is presented by Korakianitis and Wilson [30]:

$$\eta_c = 1 - \left(0.04 + \frac{r_c - 1}{150}\right) \tag{1}$$

r_c is the compressor pressure ratio. The compressor required power is calculated as below:

$$\dot{W}_c = \dot{m}_{\text{air}}(1 + \omega_1)(h_2 - h_1) \tag{2}$$

where w is the humidity ratio and h is the enthalpy.

The heat input of cycle is obtained by energy balance on combustion chamber:

$$\dot{Q}_{in} = \dot{m}_{air}(1 + \lambda)(h_3 - h_2) \quad (3)$$

where λ is the fuel to air ratio.

The gas turbine efficiency is calculated through Equation (4), as compressor efficiency [30]:

$$\eta_c = 1 - \left(0.03 + \frac{r_c - 1}{180}\right) \quad (4)$$

The turbine power generation is as follow:

$$\dot{W}_t = \dot{m}_{gas}(h_3 - h_4) \quad (5)$$

After calculating the above mentioned parameters, the net power output of the cycle is calculated:

$$\dot{W}_{net} = \dot{W}_t - \dot{W}_c \quad (6)$$

HRSG

In the proposed system a triple-pressure (LP, MP and HP) HRSG with three economizers (LP, MP and HP), three evaporators (LP, MP and HP) and a super heater (HP) is used to generate LP saturated steam, MP saturated steam and HP superheated steam. The temperature profile of HRSG is indicated in Fig. 2.

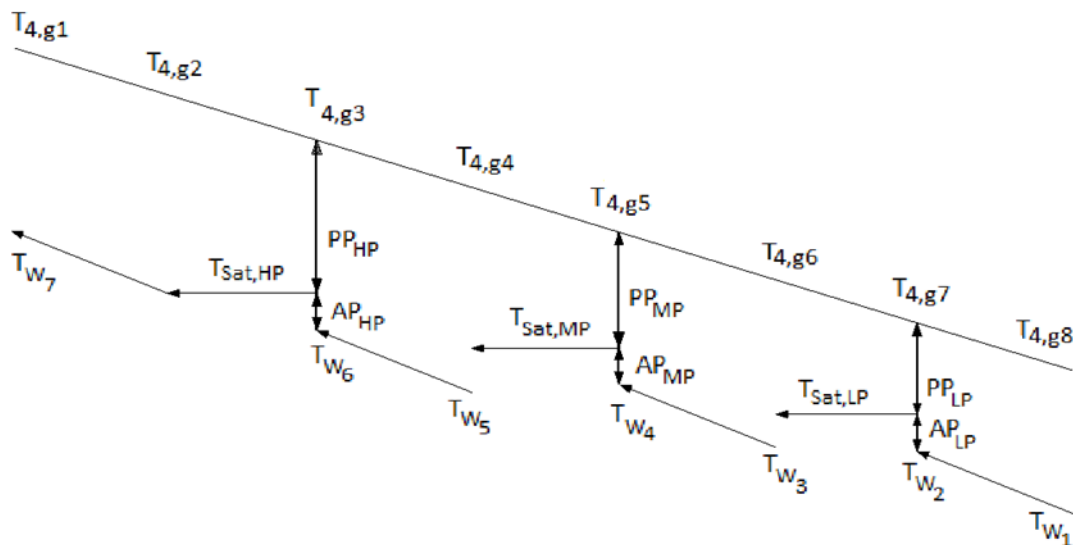


Figure 2. Temperature profile in HRSG

The pinch-point is defined as the temperature difference between the exhaust gas at the end of the evaporator (side economizer) and the saturated steam. The triple-pressure HRSG has three pinch points (PPLP, PPMP and PPHP). Also the temperature difference between the water leaving the economizers (T_{w2} , T_{w4} and T_{w6}) and the saturated steam of evaporators ($T_{sat,LP}$, $T_{sat,MP}$ and $T_{sat,HP}$) are called the approach points (APLP, APMP and APHP). The approach points depend on economizers tube layouts. Here we supposed that they are the same and equal to 5°C.

The feed water enters to LP economizer with temperature of T_{w1} and is heated to T_{w2} by extracting heat of the flue gas. The T_{w2} is calculated as follows:

$$T_{w2} = T_{sat,LP} - AP_{LP} \quad (7)$$

Similarly, T_{w4} and T_{w6} are calculated:

$$T_{w4} = T_{sat,MP} - AP_{MP} \quad (8)$$

$$T_{w6} = T_{sat,HP} - AP_{HP} \quad (9)$$

As it seen from the Fig. 2, we have:

$$T_{w3} = T_{w2} \quad (10)$$

$$T_{w5} = T_{w4} \quad (11)$$

By using the above mentioned equations, all of temperatures in water side of HRSG are found. The flue gas enters HRSG with the temperature of T_4 (or $T_{4,g1}$). $T_{4,g3}$, $T_{4,g5}$ and $T_{4,g7}$ are calculated from the Equations (12-14):

$$T_{4,g3} = T_{sat,HP} + PP_{HP} \quad (12)$$

$$T_{4,g5} = T_{sat,MP} + PP_{MP} \quad (13)$$

$$T_{4,g7} = T_{sat,LP} + PP_{LP} \quad (14)$$

$T_{4,g3}$ is the flue gas exhaust temperature from the HRSG and it is temperature that flue gas can be cold to prevent from reaching to the dew point.

By applying energy balance for the economizers of HRSG, feed water mass flow rate (or heating mass flow rate) and also $T_{4,g4}$ and $T_{4,g6}$ are obtained:

$$\dot{m}_{heating}(h_{w,1} - h_{w,2}) - \dot{m}_g(h_{4,g7} - h_{4,g8}) = 0 \quad (15)$$

$$\dot{m}_{heating}(h_{w,3} - h_{w,4}) - \dot{m}_g(h_{4,g5} - h_{4,g6}) = 0 \quad (16)$$

$$\dot{m}_{heating}(h_{w,5} - h_{w,6}) - \dot{m}_g(h_{4,g3} - h_{4,g4}) = 0 \quad (17)$$

By applying energy balance for the LP, MP and HP evaporators of HRSG (Equations (18-20)), the steam flow rate required for absorption chiller and MED_TVC and also $T_{4,g2}$ are obtained , respectively:

$$\dot{m}_5(h_{(water,Tsat,LP,x=1)} - h_{(water,Tsat,LP,x=0)}) - \dot{m}_g(h_{4,g6} - h_{4,g7}) = 0 \quad (18)$$

$$\dot{m}_{23}(h_{(water,Tsat,MP,x=1)} - h_{(water,Tsat,MP,x=0)}) - \dot{m}_g(h_{4,g4} - h_{4,g5}) = 0 \quad (19)$$

$$\dot{m}_{heating}(h_{(water,Tsat,HP,x=1)} - h_{(water,Tsat,HP,x=0)}) - \dot{m}_g(h_{4,g2} - h_{4,g3}) = 0 \quad (20)$$

Now, energy balance is applied to HP super heater of the HRSG for calculating the temperature of the superheated process steam:

$$\dot{m}_{heating}(h_{w,7} - h_{(water,Tsat,HP,x=1)}) - \dot{m}_g(h_{4,g1} - h_{4,g2}) = 0 \quad (21)$$

The amount of process heat is calculated as below:

$$\dot{Q}_{heating} = \dot{m}_{heating}(h_{w,7} - h_{w,1}) \quad (22)$$

Absorption Chiller

In the absorption chiller, mass conservation includes the mass balance of total mass and each component of the solution [31]:

$$\sum(\dot{m} \cdot x)_i - \sum(\dot{m} \cdot x)_e = 0 \quad (23)$$

\dot{m} is the mass flow rate and x is mass concentration of LiBr in the solution.

The energy balance equation is applied for each component of the absorption chiller:

- Evaporator

$$\dot{Q}_{\text{evap}} = \dot{m}_{13}(h_{16} - h_{13}) \quad (24)$$

- Absorber

$$\dot{m}_{18}x_{18} = \dot{m}_{17}x_{17} \quad (25)$$

$$\dot{Q}_{\text{abs}} = \dot{m}_{18}h_{18} - \dot{m}_{17}h_{17} - \dot{m}_{16}h_{16} \quad (26)$$

- Pump

$$\dot{W}_{\text{pump}} = \dot{m}_{18}v_{18}(P_{18} - P_{21}) \quad (27)$$

- Heat Exchanger

$$\dot{m}_{21}h_{21} + \dot{m}_8h_8 = \dot{m}_{22}h_{22} + \dot{m}_7h_7 \quad (28)$$

- Generator

$$\dot{m}_8x_8 = \dot{m}_7x_7 \quad (29)$$

$$\dot{Q}_{\text{gen}} = \dot{m}_8h_8 + \dot{m}_9h_9 - \dot{m}_7h_7 \quad (30)$$

- Condenser

$$\dot{Q}_{\text{cond}} = \dot{m}_{12}(h_{12} - h_9) \quad (31)$$

The amount of cooling capacity of the chiller is equal to the evaporator load:

$$\dot{Q}_{\text{cooling}} = -\dot{Q}_{\text{evap}} = \dot{m}_{13}(h_{13} - h_{16}) \quad (32)$$

MED-TVC Desalination Plant

The mass balance for the entire of the MED-TVC system (black box shown in Fig.3) can be performed as follows:

$$F = D_t \times \frac{x_b}{x_b - x_{sw}} \quad (33)$$

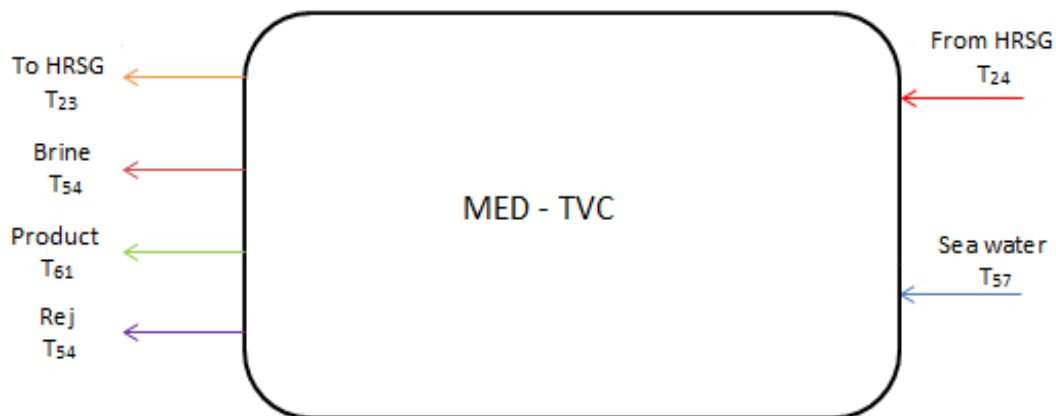


Figure 3. Entire MED-TVC system as a black

It is supposed that the mass flow rates of the effects are equal:

$$f(i) = \frac{F}{N} \quad (34)$$

$$D_t = \sum_{i=1}^N D(i) \quad (35)$$

MED system is divided into five sub-systems and mass and energy balance are applied for each of them.

- Steam ejector and de-super heater

$$R = \frac{\dot{m}_{24}}{\dot{m}_{25}} \quad (36)$$

$$h_{26} = \frac{R h_{24} + h_{25}}{1+R} \quad (37)$$

$$R_1 = \frac{\dot{m}_{63}}{\dot{m}_{24} + \dot{m}_{25}} \quad (38)$$

$$R_1 = \frac{h_{26} - h_{27}}{h_{27} - h_{63}} \quad (39)$$

$$\dot{m}_{63} = \dot{m}_{24} R_1 \left(1 + \frac{1}{R}\right) \quad (40)$$

where \dot{m}_{24} , \dot{m}_{25} and \dot{m}_{63} are the mass flow rate of the ejector motive steam, withdrawn vapor from effect n by steam ejector and water consumed in de-superheater, respectively.

Effects 1, ..., N

To have an efficient operational condition, it was supposed that the temperature difference of all effects is the same [32]:

$$\Delta T_{\text{effect}} = \left(\frac{T_s - T(N)}{N}\right) \quad (41)$$

$$T_1 = T_s - \Delta T \quad (42)$$

$$T(i+1) = T(i) - \Delta T, \quad i = 1, 2, \dots, N-1 \quad (43)$$

If $D(i)$, $B(i)$, and $f(i)$ are assumed to be the mass flow rates of steam, brine, and feed water of the i th effect, respectively and if the latent heat and the specific heat capacity of water in the i th effect are indicated by $L(i)$ and $Cp(i)$, the mass and energy balance for the effects of 1, ..., N will be as follows [33]:

Effects 1, 2 and 3

$$(\dot{m}_{24} + \dot{m}_{25} + \dot{m}_{63})L_{24} = f(i)Cp_f(T(1) - T_f(1)) + D(1)L(1) \quad (44)$$

$$(D(1) - D_r(1))L(1) + B(1)Cp_B\Delta T = f(2)Cp_f(T(2) - T_f(2)) + D(2)L(2) \quad (45)$$

$$(D(2) - D_r(2))L(2) + B(2)Cp_B\Delta T = f(3)Cp_f(T(3) - T_f(3)) + D(3)L(3) \quad (46)$$

Effects 4, ..., N

$$(D(i-1) - D_r(i-1))L(i-1) + B(i-1)Cp_B\Delta T = f(i)Cp_f(T(i) - T_f(i)) + D(i)L(i) \quad (47)$$

$$i = 4, \dots, N$$

Steam is just withdrawn in the effect N (inlet of steam ejector). Then:

$$i \neq n \rightarrow D_r(i) = 0 \quad (48)$$

$$B(i) = \sum_{i=1}^N f(i) - \sum_{i=1}^N D(i) \quad , \quad i = 1, 2, \dots, N \quad (49)$$

- Feed water heater
The energy balance for feed-water heater can be calculated as follows:

$$\sum_{i=1}^{N-1} D(i)(h_f(i) - h_f(N)) + \dot{m}_{24} \times \left[h_{f24} \left(R_1 + \frac{1+R_1}{R} \right) - \frac{h_{f24}}{R} - h_{fN} \left(R_1 + \frac{R_1}{R} \right) \right] = (f(1) + f(2) + f(3))Cp_f(T_f(1) - T_f) \quad (50)$$

- Condenser
A vapor produced in the last effect enters the condenser and condenses by seawater. Also seawater is preheated. Another part of seawater used as coolant in the condenser is rejected to the sea. The mass and energy balance for the condenser are as follows:

$$T_f = T(N) - \Delta T_{\min, \text{cond}} \quad (51)$$

$$\dot{m}_{57} = F + \text{Rej} \quad (52)$$

$$(D(N) - D_r(N))L(N) = (F + \text{Rej})Cp_{sw}(T_f - T_{sw}) \quad (53)$$

where \dot{m}_{57} , F , and Rej are the mass flow rates of condenser cooling water, feed water MED and the rejected water from desalination system, respectively. $D(N)$ is the total rate of the exhaust steam of the effect $D_r(N)$ is the rate of the withdrawn steam from the effect N . T_f and T_{sw} are the feed water and sea water temperatures, respectively. One of the most important characteristics of thermal desalination plants is gain output ratio (GOR), the ratio between the mass of produced fresh water and that of the consumed motive steam:

$$\text{GOR} = \frac{\dot{m}_{61}}{\dot{m}_{24}} \quad (54)$$

The useful load of the MED-TVC plant is obtained as follows:

$$\dot{Q}_{\text{desalination}} = \dot{m}_{61}(h_{61} - h_{sw}) \quad (55)$$

The thermal efficiency defines as the ratio of useful forms of energies produced by the system (cold, heat, power and fresh water) to the input energy of fuel that is supplied to the system. According to this definition, the efficiency for the proposed system is given by:

$$\eta_{\text{system}} = \frac{\dot{W}_{\text{net}} + \dot{Q}_{\text{heating}} + \dot{Q}_{\text{cooling}} + \dot{Q}_{\text{desalination}}}{\dot{m}_{\text{fuel}} * \text{LHV}} \quad (56)$$

where, LHV is the low heating value of the fuel (methane).

DISCUSSION AND RESULTS

Model Verification

To validate the present model and simulation results, for gas turbine cycle, absorption chiller and MED-TVC, the available data in the References [5] and [33] were used. A comparison of the simulation results with those reported in the literature, for the stand alone gas turbine cycle, absorption chiller and MED-TVC was shown in Tables 1-3. The results indicate a good agreement between the values of parameters calculated in this work and those reported in the literature.

Table 1. Performance parameters for the gas turbine cycle a) present model b) Ref. [5]

Parameters	a	b	Error (%)
Compressor isentropic efficiency	0.75	0.75	0
Turbine isentropic efficiency	0.75	0.75	0
Compressor pressure ratio	14	14	0
Gas turbine inlet temperature (°C)	1300	1300	0
Mass flow rate of fuel (kg/s)	1.21	1.21	0
Mass flow rate of air (kg/s)	87.26	81.44	-6.67
\dot{W}_{net} (kW)	19.44	19.23	-1.08
Gas turbine outlet temperature (°C)	767.4	787.53	2.62
Cycle efficiency (%)	32.11	31.78	-1.03

Table 2. Performance parameters for the absorption chiller, a) present model b) Ref. [5]

Parameters	a	b	Error (%)
Load of Evaporator (MW)	7.12	6.96	-2.25
Load of Generator (MW)	10.29	10.17	-1.17
Load of Absorber (MW)	11.36	11.05	-2.73
Load of Condenser (MW)	6.98	6.74	-3.44
COP	0.692	0.684	-1.16

Table 3. Performance parameters for the MED-TVC system a) present model b) Ref. [33]

Parameters	a	b	Error (%)
Capacity of the MED-TVC system (kg/s)	23.2	23.15	-0.22
Inlet salt composition of the sea water (%)	0.039	0.039	0
Salt composition of the outlet brine (%)	0.067	0.065	-2.99
Number of effects	7	7	0
Temperature of the vapor enters to the first effect (°C)	71	71	0
Total Steam consumption (kg/s)	2.568	2.568	0
Total feed flow rate for all effects (kg/s)	57.76	57.87	0.19
Total brine outlet flow rate (kg/s)	35.58	34.72	-2.42
Total flow rate of the inlet sea water (kg/s)	141.1	134.72	-4.52
Gain output ratio(GOR)	9.033	9.01	-0.25

Energy Analysis Result

For the considered system, the input data and assumptions are listed in Table 4. These parameters are used for the thermodynamic evaluation of the system in the base case.

Table 5 shows the thermodynamic properties as the temperature, pressure, mass flow rate, enthalpy and entropy for the points (states) of the combined cycle (see Fig.1) operating on the conditions that specified in the Table 4. The figures given in Table (5) could be helpful to evaluate streams' characteristics. The main operational and performance parameters of the considered cycles and also combined cycle are listed in Table 6.

Table 4. The input data assumed in the simulation

Parameters	Value
Gas turbine cycle	
Air compressor inlet temperature (°C)	25
Gas turbine inlet temperature (°C)	1100
Turbine isentropic efficiency	0.9
Compressor isentropic efficiency	0.85
Compressor Pressure ratio	12
Net Power of gas turbine cycle (MW)	30

Table 4. The input data assumed in the simulation (Continued)

HRSG	
Feed water temperature (°C)	25
Low pressure (kPa)	200
Medium pressure (kPa)	900
High pressure (kPa)	1500
Pinch temperature at the low pressure evaporator (°C)	50
Pinch temperature at the medium pressure evaporator (°C)	50
Pinch temperature at the high pressure evaporator (°C)	70
Approach Point at the low pressure evaporator (°C)	5
Approach Point at the low pressure evaporator (°C)	5
Approach Point at the low pressure evaporator (°C)	5
Gas temperature at the HRSG outlet (°C)	150
Gas pressure at the HRSG outlet (kPa)	101.325
Absorption Chiller	
Heat exchanger efficiency (%)	64
Cooling water inlet temperature (°C)	32.85
Cooling water outlet temperature (°C)	37.85
Weak mass concentration of LiBr	57
Strong mass concentration of LiBr	64
MED-TVC system	
Sea water inlet temperature (°C)	35
Salt composition of the sea water Inlet (%)	0.039
Salt composition of the brine outlet (%)	0.067
Number of effects	7
Temperature of the vapor to the first effect (°C)	71
Temperature of the last effect (°C)	48
Motive steam/return vapor in the TVC (R)	1.9
Minimum temperature difference in the condenser (°C)	3
Temperature difference between effects (°C)	3.286

Table 5. Thermodynamic properties of the streams for a typical operating condition

Stream	T (K)	P (kPa)	\dot{m} (kg/s)	h (kJ/kg)	s (kJ/kgK)	X (%)	x (%)
1	298.15	101.3	106.4	298.6	5.695	-	-
2	651.75	1216	106.4	662	5.783	-	-
3	1375.15	1106	107.6	601.6	7.996	-	-
4	841.25	109.3	107.6	-36.53	8.084	-	-
5	393.35	200	1.989	2707	7.127	-	-
6	393.35	200	1.989	504.7	1.53	-	-
7	311.5	7.322	14.06	99.06	0.2241	-	57
8	313	7.322	12.53	144.9	0.2123	-	64
9	313	7.322	1.538	2573	8.258	-	-
10	306	4.991	177	137.6	0.4757	-	-
11	311	6.576	177	158.5	0.5435	-	-
12	313	7.322	1.538	166.9	0.5703	-	-
13	278.65	0.9034	1.538	166.9	0.5997	-	-
14	285	1.389	172.1	49.73	0.1782	-	-

Table 5. Thermodynamic properties of the streams for a typical operating condition (Continued)

Stream	T (K)	P (kPa)	\dot{m} (kg/s)	h (kJ/kg)	s (kJ/kgK)	X (%)	x (%)
15	280	0.9918	172.1	28.79	0.1041	-	-
16	278.65	0.9034	1.538	2511	9.011	-	-
17	311.08	0.9034	12.53	141.6	0.2015	-	64
18	310	0.9034	14.06	96.1	0.2145	-	57
19	306	4.991	204.8	137.6	0.4757	-	-
20	311	6.576	204.8	158.5	0.5435	-	-
21	310	7.322	14.06	96.1	0.2145	-	57
22	311.08	7.322	12.53	141.6	0.2015	-	64
23	448.55	900	1.924	742.8	2.095	-	-
24	448.55	900	1.924	2774	6.622	-	-
25	327.71	15.44	1.012	2599	7.997	-	-
26	388.25	32.93	2.936	2713	7.968	-	-
27	344.15	32.93	3.04	2628	7.739	-	-
28	329.4	28.98	6.185	223.8	0.7442	0.039	-
29	340.85	28.24	3.278	258.1	0.8302	0.073	-
30	344.15	32.59	3.04	297.2	0.9671	-	-
31	340.85	28.24	2.907	2622	7.788	-	-
32	329.4	24.4	6.147	223.8	0.7442	0.039	-
33	337.56	24.4	2.828	2616	7.839	-	-
34	337.56	24.4	6.597	245.7	0.7943	0.072	-
35	340.85	28.24	2.907	283.4	0.9268	-	-
36	329.4	21.02	6.227	223.8	0.7442	0.039	-
37	334.28	21.02	2.802	2611	7.89	-	-
38	334.28	21.02	10.02	233	0.7565	0,072	-
39	337.56	24.4	2.828	269.6	0.8862	-	-
40	318.15	18.05	6.162	178,8	0.6054	0.039	-
41	330.99	18.05	2.711	2605	7.943	-	-
42	330.99	18.05	13.47	220.6	0.7198	0.071	-
43	334.28	21.02	2.802	255.9	0.8453	-	-
44	318.15	15.44	6.221	178.8	0.6054	0.039	-
45	327.71	15.44	1.663	2599	7.997	-	-
46	327.71	15.44	17.02	207.9	0.6812	0.071	-
47	330.99	18.05	2.711	242.1	0.804	-	-
48	318.15	13.16	6.245	178.8	0.6054	0.039	-
49	324.42	13.16	1.686	2593	8.053	-	-
50	324.42	13.16	21.58	195.8	0.645	0.069	-
51	327.71	15.44	1.663	228.4	0.7623	-	-
52	318.15	11.18	6.09	178.8	0.6054	0.039	-
53	321.13	11.18	1.766	2588	8.11	-	-
54	321.13	11.18	25.9	183.5	0.6082	0.067	-
55	324.42	13.16	1.686	214.6	0.7201	-	-
56	321.13	11.18	1.766	200.9	0.6776	-	-
57	308.15	29	105.7	138.9	0.478	0.039	-
58	318.15	29	105.7	178.8	0.6054	0.039	-
59	318.15	29	18.56	178.8	0.6054	0.039	-

Table 5. Thermodynamic properties of the streams for a typical operating condition (Continued)

Stream	T (K)	P (kPa)	\dot{m} (kg/s)	h (kJ/kg)	s (kJ/kgK)	X (%)	x (%)
60	333.19	20	17.37	251.3	0.8317	-	-
61	321.71	20	17.37	203.3	0.685	-	-
62	329.4	29	18.56	223.8	0.7442	0.039	-

Table 6. Performance parameters of the considered systems

Parameters	Value
Gas turbine cycle	
Fuel flow rate (kg/s)	1.149
Air flow rate (kg/s)	99.76
Compressor power consumption (MW)	38.666
HRSG	
LP saturated steam flow rate (kg/s)	1.785
MP saturated steam flow rate (kg/s)	1.845
HP superheated steam flow rate (kg/s)	5.04
HP superheated steam temperature (°C)	336.1
\dot{Q}_{heating} (MW)	14.179
Absorption Chiller	
$\dot{Q}_{\text{Evaporator}}$ (MW)	3.434
$\dot{Q}_{\text{Condenser}}$ (MW)	3.834
$\dot{Q}_{\text{Absorber}}$ (MW)	4.585
$\dot{Q}_{\text{Generator}}$ (MW)	4.063
COP	0.845
Desalination	
Capacity of the MED-TVC system (kg/s)	16.12
Product average temperature before the feed water heater (°C)	60.04
$\dot{Q}_{\text{Desalination}}$ (MW)	1.038
Gain output ratio (GOR)	9.033
Water consumption in the de-superheater (kg/s)	0.09615
Total Steam consumption (kg/s)	1.785
Total feed flow rate for all effects (kg/s)	40.15
Combined system	
Efficiency of the system (%)	84.6

PARAMETRIC STUDY

In this section, the effects of the important operational parameters such as compressor pressure ratio, gas turbine inlet temperature, pressures (LP, MP and HP) of the drums of the HRSG, LP, MP and HP pinch points and the temperature differences between the effects of the MED are considered for the parametric study of the proposed system performance.

Effects of the Compressor Pressure Ratio

The changes in cooling, heating and fresh water productions, fuel consumption and also efficiency of the system with the variation of air compressor pressure ratio (r_c) are shown in Fig. 4. As pressure ratio increases, the fuel consumption decreases. This is because of the increase of the air temperature and flow rate that enters the combustion chamber. Namely, when the inlet air energy increases, less fuel is consumed to meet the energy balance necessities (see Fig. 4a). The compressor power consumption and turbine power generation increase at high

pressure ratios. Because the net power of gas turbine cycle has been assumed to be constant, then this phenomenon has no effect on the net power generation. By increasing the pressure ratio, cooling and fresh water productions decrease at first and then increase. This phenomenon is because of the variations of the passing gas over the low and medium pressure evaporators and consequently variations of the vapor productions of these evaporators (see Fig. 4b and c). The heating power of the plant decreases because of the decrement of the passing gas over the high pressure superheater (see Fig. 4b). All of these effects tend to increment of the system efficiency with the increase of the air compressor pressure ratio (see Fig. 4d).

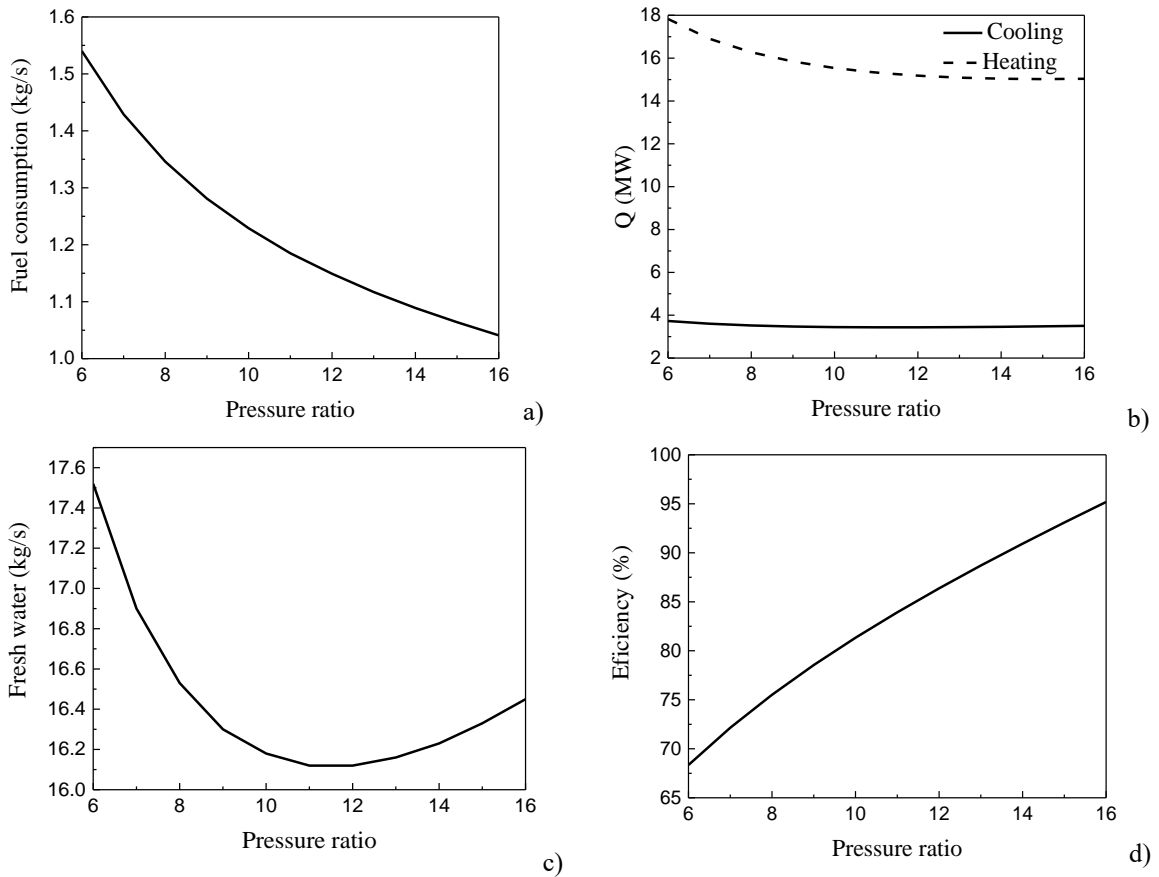
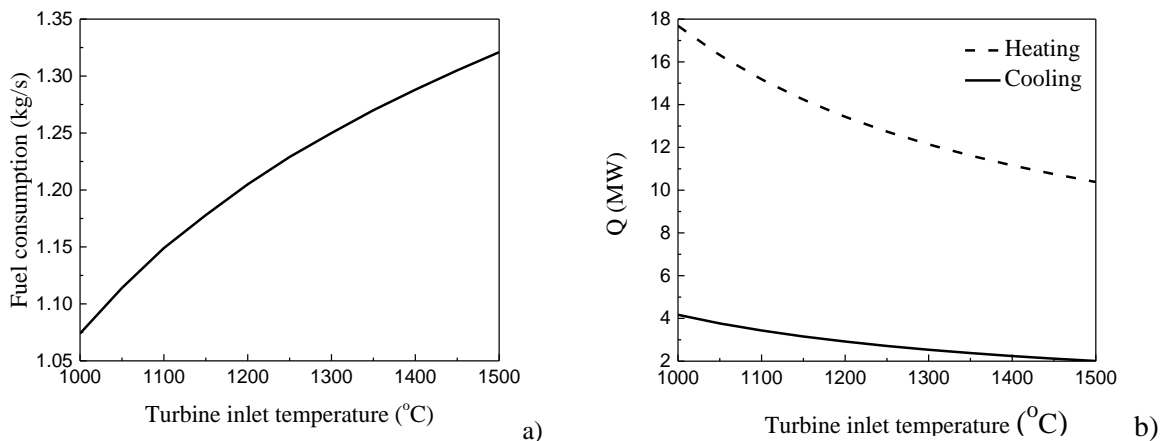


Figure 4. Effects of the variation of the compressor pressure ratio on the thermodynamic parameters (other parameters are in base case)

Effects of the Turbine Inlet Temperature

Fig. 5 shows the variations of cooling, heating and fresh water productions, fuel consumption and efficiency of the system with respect to the changes of the turbine inlet temperature.



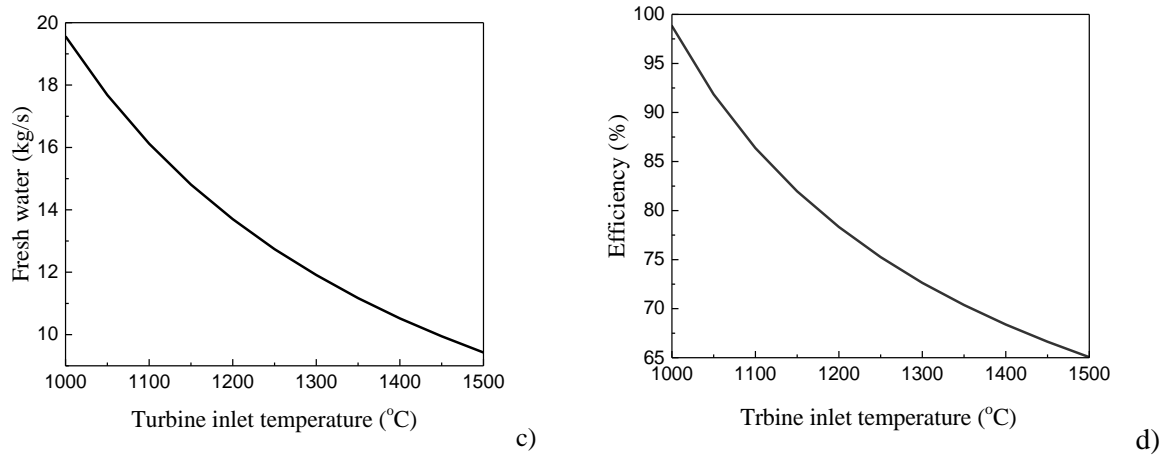


Figure 5. Effects of the variation of the turbine inlet temperature on the thermodynamic parameters (other parameters are in base case)

As the turbine inlet temperature increases, considering energy balance in the combustion chamber, the fuel consumption increases (see Fig. 5 a). But because of the constant net power generation (30 MW), the flow rate of air that enters combustion chamber decreases. The decrement of air flow rate much more than fuel consumption. Then the amount of the energy of the inlet and also outlet gas of the turbine decreases. Consequently, heating, cooling and fresh water productions decrease and also the system efficiency decrease with respect to the increment of the turbine inlet temperature (see Fig. 5 b, c and d).

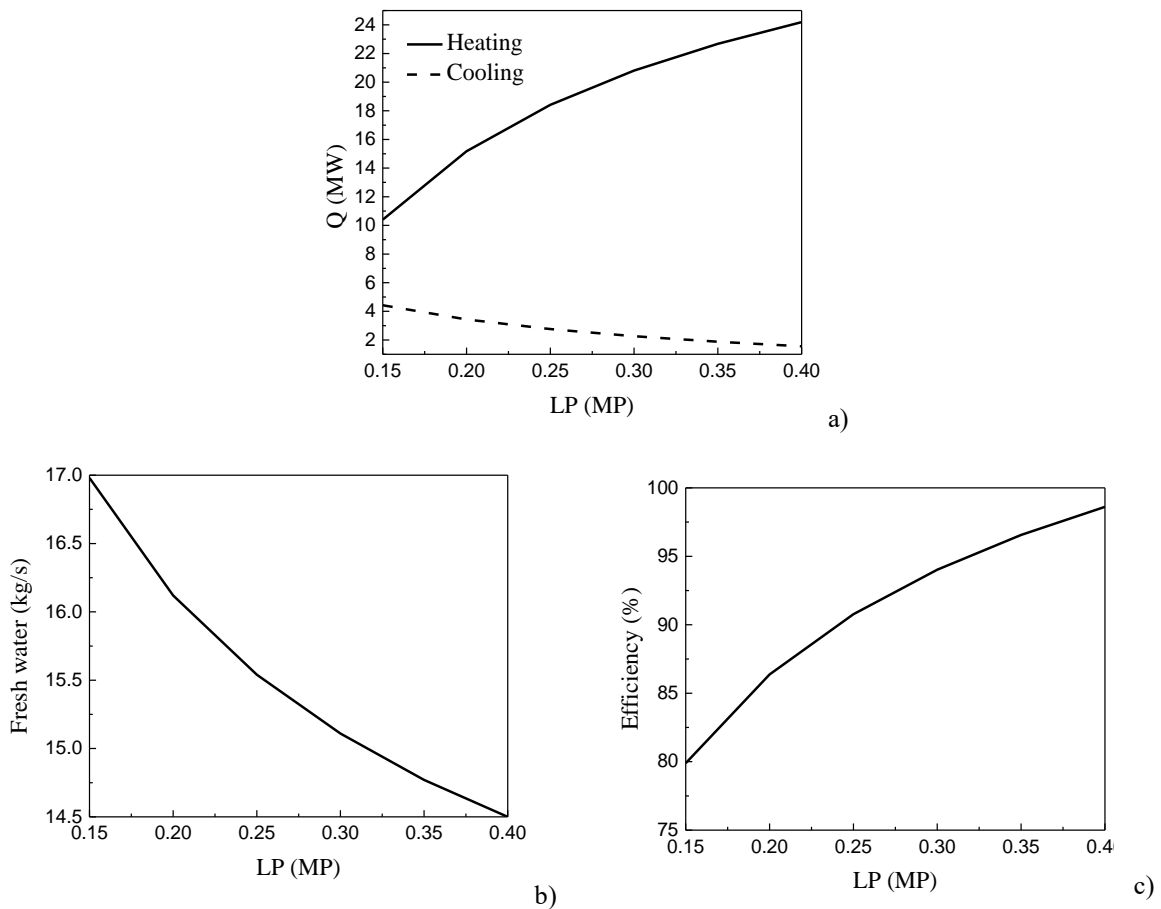


Figure 6. Effects of the variation of the LP on the thermodynamic parameters (other parameters are in base case)

Effects of Variations of the Pressure in LP Evaporator of the HRSG

The variation of the LP has no effect on the fuel consumption. Combustion is occurred in the combustion chamber and just the energy of the turbine exhaust gas is recovered in the HRSG. Then the variation of pressures in the evaporators of the HRSG has not any effect on the fuel consumption. By increasing the LP, the saturation temperature in the LP evaporator of the HRSG and also the LP evaporator outlet gas temperature increase (Eq. (14)). This effect tends to the increment of the heating flow rate Eq. (15) and also amount of the heating (see Fig.6 a). Conversely, LP increment tends to the decrement of the steam flow rates that are needed for the absorption chiller and also MED-TVC (Eqs. (18) and (19)). Then amount of cooling and fresh water productions are decreased (see Fig.6a and b). Whereas the increment of the heating power is much more than the cooling and fresh water productions, then the system efficiency increases as the increment of the LP (see Fig.6 c).

Effects of Variations of the Pressure in MP Evaporator of the HRSG

Fuel consumption remains constant with changes in MP. As mentioned in the previous section, the variation of the HRSG’s pressures has no effect on the fuel consumption.

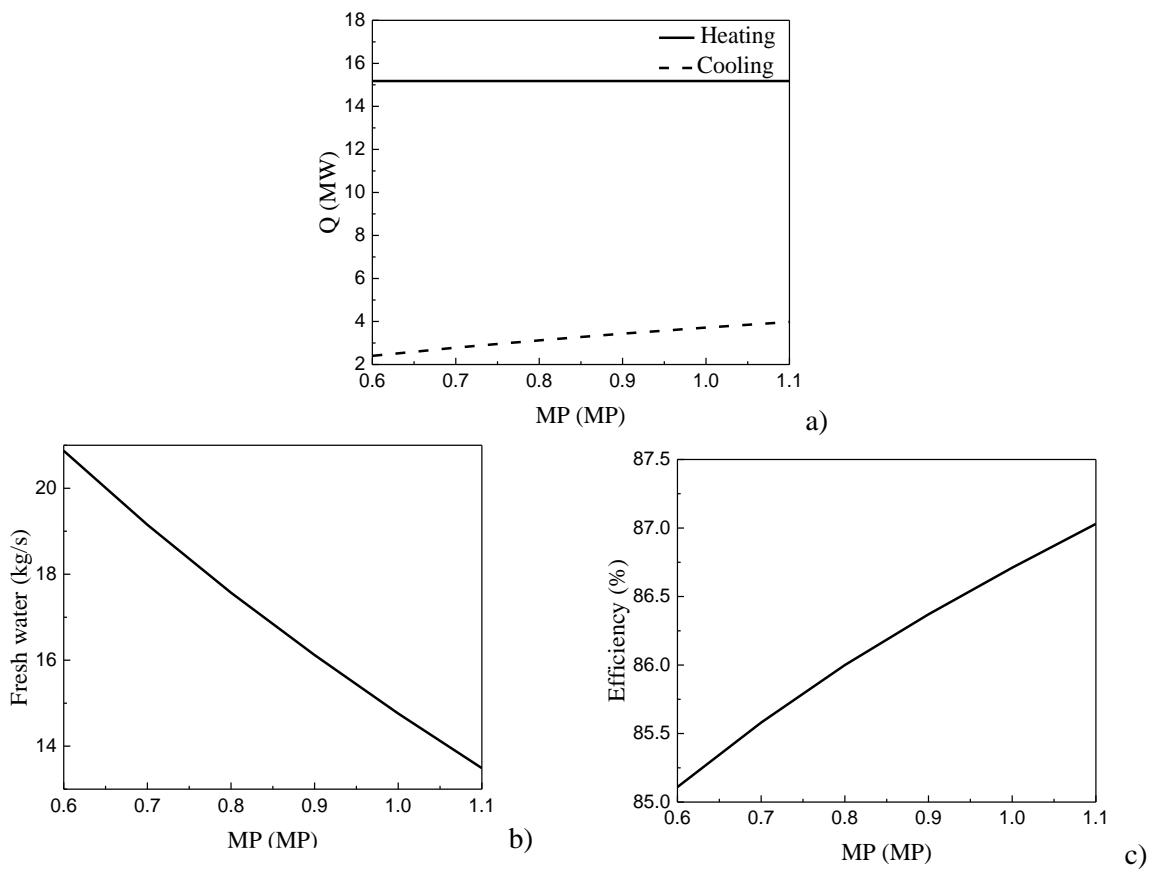


Figure 7. Effects of the variation of the MP on the thermodynamic parameters (other parameters are in base case)

The MP increment leads to increment of the outlet gas temperature of the MP evaporator (Eq. 13) and also MP economizer outlet water temperature (Eq.8). Since water and gas temperatures of LP economizer and evaporator and also HP evaporator and superheater remain constant, the heating flow rate (Eq.15) and temperature (Eq.21) do not change with the increment of the MP (see Fig.7 a). But increasing of the MP decreases the cooling and fresh water productions because of the decrement of the amount of the steam productions in LP and MP evaporators, respectively (see Fig.7a and b). Consequently, the system efficiency increases slightly by the increment of the MP (see Fig.7 c).

Effects of the Variations of the Pressure in HP Evaporator of the HRSG

The variation of the HP has no effect on the cooling power of the plant (see Fig.8 a). Because HP increments does not affect the LP economizer and evaporator inlet and outlet flows. Then heating flow rate remains

constant (Eq. 15). On the other hand HP increment increases the inlet gas temperature of the MP evaporator (Eq. 17) that tends to the increment of the amount of the steam that runs the MED-TVC (Eq. 19). Then fresh water production increases (see Fig.8 b). Although the HP steam flow rate remains constant, but the superheat steam temperature decreases slightly (Eq. 21) and tends to the decrement of the heating power (see Fig. 8 a). These effects all tend to the increment of the system efficiency with the increment of the HP (see Fig.8 c).

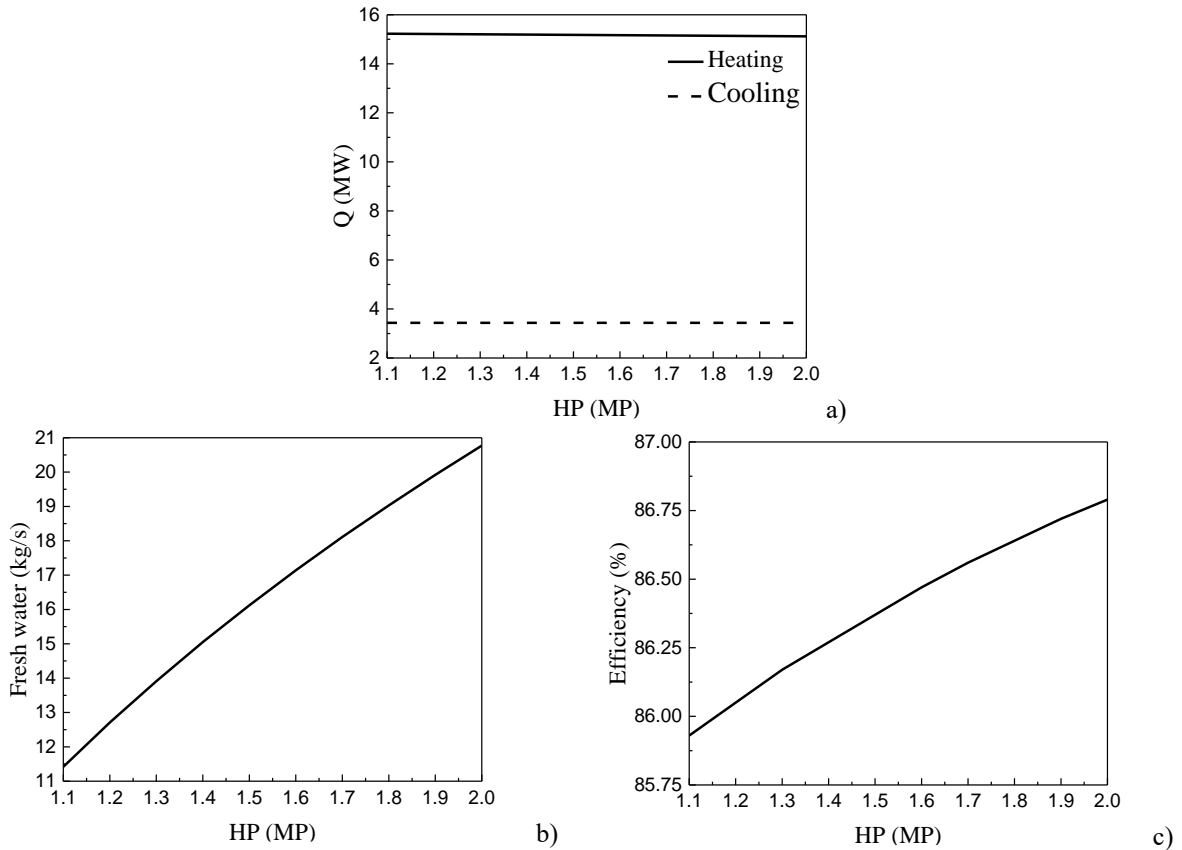
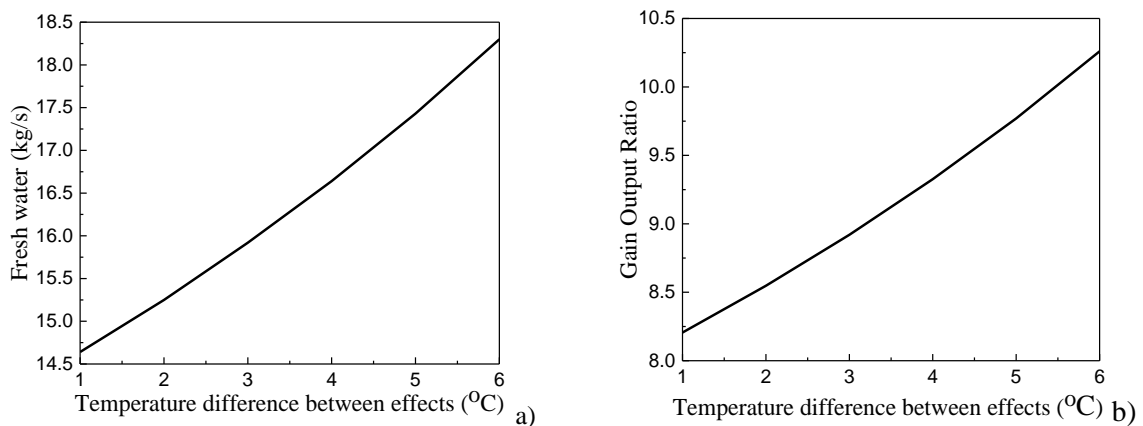


Figure 8. Effects of the variation of the HP on the thermodynamic parameters (other parameters are in base case)

Effects of the Variations of the Temperature Difference between the Effects on the Performance of the MED-TVC

By increasing the temperature difference between the effects, the temperature and also the pressure of the next effect decreases (Eq. 43). In this condition the heat transfer from the motive steam increases and tends to the increment of the fresh water production and also GOR (see Fig.9a and b). Then the system efficiency increases (see Fig 9 c). It also leads to the decrement of the product average temperature (see Fig 9 d).



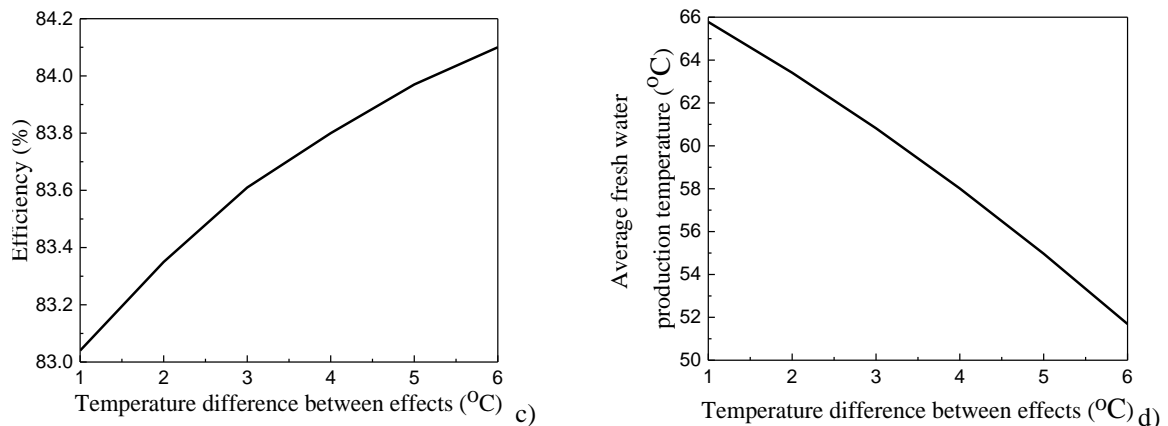


Figure 9. Effects of the variation of the temperature difference between the effects on the performance of the MED-TVC (other parameters are in base case)

CONCLUSIONS

In this research paper, a comprehensive thermodynamic model of a new integrated multi-generation (cooling, heating, power and potable water) system was carried out. In this system a multi effect distillation thermal vapor compression (MED-TVC) was integrated in a combined cooling, heating and power (CCHP) system with gas turbine prime mover. For this integration a triple pressure heat recovery steam generator (HRSG) was used. The low pressure and medium pressure of the HRSG were used to the handling of an absorption chiller for cooling and a MED-TVC desalination system for potable water production, respectively. Also the high pressure superheated steam was used for process utilities, directly. A systematic investigation of the effects of system parameters on performance such as system efficiency, cooling and heating power, potable water production and gain output ratio of the MED system was done. It is found that, the efficiency of the integrated system reached to 84%, whereas the gas turbine efficiency was 32%. With increasing of the compressor pressure ratio, the system efficiency, fuel consumption and heating power have ascending trend. But the cooling power and fresh water production decrease at first and after getting a minimum value then increase. By increasing the turbine inlet temperature, the fuel consumption increases, whereas the cooling and heating power and also the fresh water productions and the system efficiency decrease. The pressures (LP, MP and HP) of the HRSG has no effect on the fuel consumption. Also heating and cooling power are constant with the variations of the MP and HP, respectively. The cooling power and fresh water production increase with the increment of the LP and MP whereas increment of the HP cause to the increment of the fresh water production. The heating power increases when the LP decreases and HP increases. It is found that the system efficiency has an ascending trend with the increment of all the above mentioned parameters (LP, MP and HP). It is also concluded that by increasing the temperature difference in the effects of the MED-TVC desalination plant, the fresh water production and gain output ratio (GOR) increase and the product outlet temperature decreases.

NOMENCLATURE

AP	Approach Point (°C)
B	Brine
C_p	Specific heat capacity (kJ/kgK)
D	Distillate at desalination (kg/s)
$D_{i(i)}$	Distillate from the i^{th} effect (kg/s)
F	Total feed flow rate of MED-TVC (kg/s)
F	Feed water of desalination effects (kg/s)
GOR	Gain Output Ratio
HP	High Pressure (MPa)
H	Enthalpy (kJ/kg)
L	Latent heat (kJ/kg°C)
LHV	Low Heating value (kJ/kg)
LP	Low Pressure (MPa)

\dot{m}	Mass flow rate (kg/s)
MP	Medium Pressure (MPa)
PP	Pinch Point (°C)
\dot{Q}	Heat (MW)
R	Pressure ratio
Rej	Sea water reject (kg/s)
T	Temperature (°C)
\dot{W}	Power (MW)
X	Mass concentration (%)

Greek Symbols

H	Efficiency (%)
ω	Humidity ratio
λ	Fuel to air ratio
ΔT	Temperature difference (°C)

Subscripts

a	Air
abs	Absorber
evap	Evaporator
f	Fluid
fuel	Fuel
I	Inlet
Gen	Generator
G	Gas
HP	High pressure
LiBr	Lithium bromide
LP	Low pressure
MP	Medium pressure
P	Product
S	First effect desalination inlet
sh	Super heater
sat,LP	Low pressure saturation
sat,MP	Medium pressure saturation
sat,HP	High pressure saturation
sat	Saturation
sw	Sea water
t	Turbine

REFERENCES

- [1] Dincer, I. (2000). Renewable energy and sustainable development: a crucial review. *Renewable and sustainable energy reviews*, 4(2), 157-175.
- [2] Dincer, I., & Rosen, M. A. (1998). A worldwide perspective on energy, environment and sustainable development. *International Journal of Energy Research*, 22(15), 1305-1321.
- [3] Dincer, I. (1998). Energy and environmental impacts: present and future perspectives. *Energy sources*, 20(4-5), 427-453.
- [4] Dincer, I., & Rosen, M. A. (1999). Energy, environment and sustainable development. *Applied energy*, 64(1-4), 427-440.
- [5] Ghaebi, H., Amidpour, M., Karimkashi, S., & Rezayan, O. (2011). Energy, exergy and thermoeconomic analysis of a combined cooling, heating and power (CCHP) system with gas turbine prime mover. *International Journal of Energy Research*, 35(8), 697-709.

- [6] Ghaebi, H., Saidi, M. H., & Ahmadi, P. (2012). Exergoeconomic optimization of a trigeneration system for heating, cooling and power production purpose based on TRR method and using evolutionary algorithm. *Applied thermal engineering*, 36, 113-125.
- [7] Orhan, M. F., Dincer, I., Naterer, G. F., & Rosen, M. A. (2010). Coupling of copper–chloride hybrid thermochemical water splitting cycle with a desalination plant for hydrogen production from nuclear energy. *International Journal of Hydrogen Energy*, 35(4), 1560-1574.
- [8] Uche, J., Serra, L., & Valero, A. (2001). Thermo-economic optimization of a dual-purpose power and desalination plant. *Desalination*, 136(1-3), 147-158.
- [9] Zamen, M., Amidpour, M., & Soufari, S. M. (2009). Cost optimization of a solar humidification–dehumidification desalination unit using mathematical programming. *Desalination*, 239(1-3), 92-99.
- [10] Wang, Y., & Lior, N. (2006). Performance analysis of combined humidified gas turbine power generation and multi-effect thermal vapor compression desalination systems—Part 1: The desalination unit and its combination with a steam-injected gas turbine power system. *Desalination*, 196(1-3), 84-104. [11] J. Johansen, R.F. Babus'Haq, S.D. Probert, An integrated CHP and desalination plant, *Appl. Energy* 53 (1996) 157–178.
- [12] Wade, N. M. (1999). Energy and cost allocation in dual-purpose power and desalination plants. *Desalination*, 123(2-3), 115-125.
- [13] Cardona, E., & Piacentino, A. (2004). Optimal design of cogeneration plants for seawater desalination. *Desalination*, 166, 411-426.
- [14] Darwish, M. A. (2004). Co-generation power desalting plants: new outlook with gas turbines. *Desalination*, 161(1), 1-12.
- [15] Rensonnet, T., Uche, J., & Serra, L. (2007). Simulation and thermo-economic analysis of different configurations of gas turbine (GT)-based dual-purpose power and desalination plants (DPPDP) and hybrid plants (HP). *Energy*, 32(6), 1012-1023.
- [16] Wang, Y., & Lior, N. (2006). Performance analysis of combined humidified gas turbine power generation and multi-effect thermal vapor compression desalination systems—Part 1: The desalination unit and its combination with a steam-injected gas turbine power system. *Desalination*, 196(1-3), 84-104.
- [17] Wang, Y., & Lior, N. (2007). Performance analysis of combined humidified gas turbine power generation and multi-effect thermal vapor compression desalination systems—Part 2: The evaporative gas turbine based system and some discussions. *Desalination* 207, 243–256.
- [18] Chacartegui, R., Sanchez, D., Di Gregorio, N., Jiménez-Espadafor, F. J., Munoz, A., & Sanchez, T. (2009). Feasibility analysis of a MED desalination plant in a combined cycle based cogeneration facility. *Applied thermal engineering*, 29(2-3), 412-417.
- [19] Manesh, M. K., & Amidpour, M. (2009). Multi-objective thermo-economic optimization of coupling MSF desalination with PWR nuclear power plant through evolutionary algorithms. *Desalination*, 249(3), 1332-1344.
- [20] Ansari, K., Sayyaadi, H., & Amidpour, M. (2010). Thermo-economic optimization of a hybrid pressurized water reactor (PWR) power plant coupled to a multi effect distillation desalination system with thermo-vapor compressor (MED-TVC). *Energy*, 35(5), 1981-1996.
- [21] Hosseini, S. R., Amidpour, M., & Behbahaninia, A. (2011). Thermo-economic analysis with reliability consideration of a combined power and multi stage flash desalination plant. *Desalination*, 278(1-3), 424-433.
- [22] Hosseini, S. R., Amidpour, M., & Shakib, S. E. (2012). Cost optimization of a combined power and water desalination plant with exergetic, environment and reliability consideration. *Desalination*, 285, 123-130.
- [23] Shakib, S. E., Amidpour, M., & Aghanajafi, C. (2012). A new approach for process optimization of a METVC desalination system. *Desalination and Water Treatment*, 37(1-3), 84-96.
- [24] Shakib, S. E., Amidpour, M., & Aghanajafi, C. (2012). Simulation and optimization of multi effect desalination coupled to a gas turbine plant with HRSG consideration. *Desalination*, 285, 366-376.
- [25] Esfahani, I. J., & Yoo, C. (2014). Feasibility study and performance assessment for the integration of a steam-injected gas turbine and thermal desalination system. *Desalination*, 332(1), 18-32.
- [26] Almutairi, A., Pilidis, P., Al-Mutawa, N., & Al-Weshahi, M. (2016). Energetic and exergetic analysis of cogeneration power combined cycle and ME-TVC-MED water desalination plant: Part-I operation and performance. *Applied Thermal Engineering*, 103, 77-91.
- [27] Hanafi, A. S., Mostafa, G. M., Fathy, A., & Waheed, A. (2015). Thermo-economic analysis of combined cycle MED-TVC desalination system. *Energy Procedia*, 75, 1005-1020.
- [28] Sanaye, S., & Asgari, S. (2013). Four E analysis and multi-objective optimization of combined cycle power plants integrated with Multi-stage Flash (MSF) desalination unit. *Desalination*, 320, 105-117.
- [29] Bejan, A., & Tsatsaronis, G. (1996). *Thermal design and optimization*. John Wiley & Sons.
- [30] Korakianitis, T., & Wilson, D. G. (1994). Methods for prediction the performance of Brayton-cycle engines. *ASME Journal of Engineering for Gas Turbines and Power*, 116, 381–388.
- [31] Herold, K. E., Radermacher, R., & Klein, S. A. (2016). *Absorption chillers and heat pumps*. CRC press.
- [32] Kamali, R. K., Abbassi, A., & Vanini, S. S. (2009). A simulation model and parametric study of MED–TVC process. *Desalination*, 235(1-3), 340-351.

- [33] Sayyaadi, H., & Saffari, A. (2010). Thermoeconomic optimization of multi effect distillation desalination systems. *Applied Energy*, 87(4), 1122-1133.